18th INTERNATIONAL SYMPOSIUM on POWER ELECTRONICS - Ee 2015

NOVI SAD, SERBIA, October 28th - 30th, 2015

AN INTEGRATED MULTIPHASE SYSTEM FOR SLOW AND FAST EV BATTERY CHARGING

I. Subotic, N. Bodo, E. Levi, B. Dumnic*, D. Milicevic*, V. Katic*

School of Engineering, Technology and Maritime Operations, Liverpool John Moores University, Liverpool L3 3AF, UK

* Faculty of Technical Sciences, University of Novi Sad, 21000 Novi Sad, Republic of Serbia

Abstract: *The paper considers an on-board charger for electric vehicles (EVs). The charger is capable of both multiphase (fast) and single-phase (slow) charging. Instead of being placed on-board as a separate unit, the charger reutilizes existing components that can be found in EVs, and that are usually used only for the propulsion. These are primarily a six-phase inverter and an asymmetrical six-phase machine. During the charging mode a torque is not produced in the machine, so that the rotor does not need to be mechanically locked. Hardware reconfiguration between propulsion and slow charging mode is not required. Fast charging requires hardware reconfiguration according to the principles of phase transposition. In the paper the integrated topology is explained, and its operating principles and equivalent scheme elaborated. Experimental verification of theoretical results is provided for multiphase and singe-phase charging as well as for the single-phase V2G (vehicle-to-grid) mode.*

Key Words: ***Battery Chargers, Electric Vehicles, Integrated On-Board Chargers, Six-Phase Machines***

1. INTRODUCTION

An area of EVs that is recently getting lots of attention is charging. The main challenge is to make an infrastructure that would be capable to stand high charging demands that will inevitably be seen in the near future, with the increase of the number of EVs. A part of the problem is that a high number of fast charging stations has to be installed and, considering a high cost of a typical modern dc charging station, this is not an easy task. One possible solution is to equip vehicles with on-board chargers, and then to make an infrastructure of points where ac mains is accessible. The problem is that on-board chargers as standalone devices are not capable of fast charging. Nonetheless, increasing their power rating substantially is not viable, since it would load the vehicle with unacceptably high weight and would increase the cost significantly. Fortunately, the power electronics components that are required for rectification of ac voltages and power electronics components that are used in EVs for propulsion are very similar and are never used at the same time. First proposals of integrating these two came more than thirty years ago [1]. At present, integrated chargers are seen as one of the main potential solutions to the mass charging problem.

Although numerous proposals for integration have already been introduced [2], the majority of them are restricted to single-phase charging. The main reason for this is that it is easy to avoid a torque production in the machine during the single-phase charging process. On the other hand, single-phase charging is restricted by the low maximum power that can be taken from single-phase mains; thus the charging process is very slow.

Some of the integrated fast charging solutions can be found in [3-9]. Probably the one with the greatest potential is [3] and it is currently considered for utilization in future EVs by Valeo [10].

This paper considers an integrated charger based on integration of a six-phase machine and a six-phase inverter. It is organised as follows. In Section 2 topology capable of slow and fast charging is introduced and its operating principles assessed at a theoretical level. Equivalent schemes for charging/V2G mode of operation are given in Section 3. In Section 4 experimental results are reported in order to validate the theoretical considerations. Experimental results are provided for both slow and fast charging topology.

2. THEORETICAL CONSIDERATIONS

Single-phase charging is inferior to the fast charging, mainly due to the reduced maximum charging power when compared to the three-phase or multiphase system, which prolongs the charging process. However, if a vehicle has already a three-phase or a multiphase charger, it is desirable that it also has an integrated single-phase charger. It can provide its user with additional charging options, considering that the single-phase sockets are much more widely spread than the three-phase (and multiphase) ones.

Figs. 1 and 2 show the topology studied here for a multiphase (fast) and single-phase (slow) charging. Fast charger contains a transformer with two secondaries. Its function is to provide isolation, as well as a set of six-

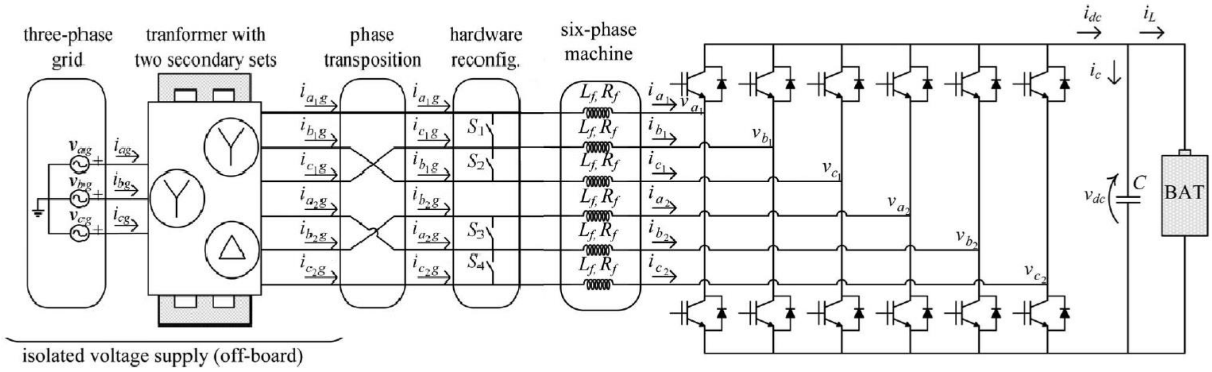

Fig. 1. *Topology of fast integrated on-board battery charger.*

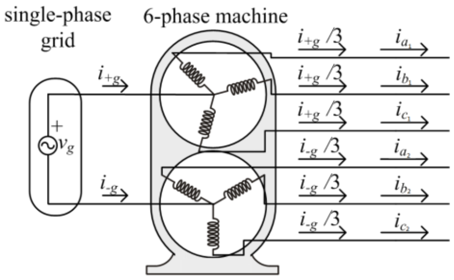

Fig. 2. *Connection diagram of slow integrated on-board battery charger (right-hand side of Fig. 2 is the same as in Fig. 1).*

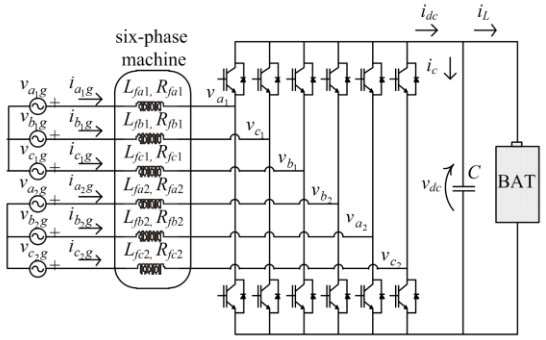

Fig. 3. *Equivalent scheme of the fast integrated six-phase charger from Fig. 1.*

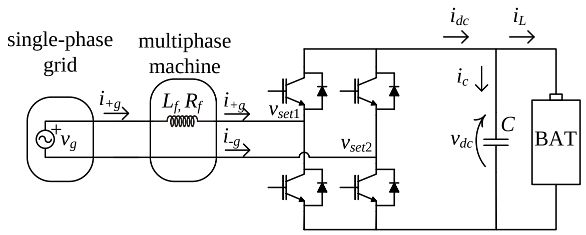

Fig. 4. *Equivalent scheme of slow integrated battery charger from Fig. 2.*

phase voltages. Transformer secondary terminals are connected to the machine in accordance with the phase transposition principle [11] in order to avoid torque production in the machine. Thus, hardware reconfiguration is required to open the machine's neutral points and connect machine phases to the transformer.

On the other hand, single-phase charging does not require hardware reconfiguration. The connection to the grid is shown in Fig. 2, while the right part is the same as in Fig. 1.

In order to assess if torque is produced in the machine during the fast or slow charging process, a decoupling matrix for the multiphase system has to be considered.

2.1. Fast charging

The decoupling transformation matrix for the asymmetrical six-phase systems is available in [12]. Its application yields 2D components in two orthogonal planes, which can be given using complex space vectors as:

$$\begin{aligned} \underline{f}_{\alpha\beta} &= \sqrt{2/6}\left(f_{a_1} + \underline{a}^4 f_{b_1} + \underline{a}^8 f_{c_1} + \underline{a} f_{a_2} + \underline{a}^5 f_{b_2} + \underline{a}^9 f_{c_2}\right) \\ \underline{f}_{xy} &= \sqrt{2/6}\left(f_{a_1} + \underline{a}^8 f_{b_1} + \underline{a}^{16} f_{c_1} + \underline{a}^5 f_{a_2} + \underline{a} f_{b_2} + \underline{a}^9 f_{c_2}\right) \end{aligned} \quad (1)$$

where $\underline{a} = \exp(j\delta) = \cos\delta + j\sin\delta$ and $\delta = \pi/6$. Symbol f stands for any variable that is being transformed (e.g. current, voltage, etc.), α-β are components in the torque-producing plane, and x-y are components in the second (non-torque producing) plane.

Zero-sequence components are given with:

$$\begin{aligned} f_{0+} &= \sqrt{2/6}(f_{a1} + f_{b1} + f_{c1}) \\ f_{0-} &= \sqrt{2/6}(f_{a2} + f_{b2} + f_{c2}) \end{aligned} \quad (2)$$

Grid currents at the secondary are governed with:

$$\begin{aligned} i_{k_1 g} &= \sqrt{2}I\cos(\omega t - l\pi/6) \quad l = 0,4,8 \quad k_1 = a_1, b_1, c_1 \\ i_{k_2 g} &= \sqrt{2}I\cos(\omega t - l\pi/6) \quad l = 1,5,9 \quad k_2 = a_2, b_2, c_2 \end{aligned} \quad (3)$$

From Fig. 1 it can be seen that the correlation of secondary currents and the currents that flow through the asymmetrical six-phase machine is:

$$\begin{aligned} i_{a_1} &= i_{a_1 g} \quad i_{b_1} = i_{c_1 g} \quad i_{c_1} = i_{b_1 g} \\ i_{a_2} &= i_{b_2 g} \quad i_{b_2} = i_{a_2 g} \quad i_{c_2} = i_{c_2 g} \end{aligned} \quad (4)$$

Substitution of (3) and (4) into (1) leads to the following two space vectors:

$$\underline{i}_{\alpha\beta} = 0 \quad (5)$$

$$\underline{i}_{xy} = \sqrt{6}I\exp(j\omega t) \quad (6)$$

Clearly, the flux/torque producing plane (α-β) is not excited and the grid currents flow through the x-y plane, so that the machine stays at standstill. Zero-sequence components are both equal to zero.

2.2. Slow charging

If slow charging is considered, the decoupling matrix remains the same and is hence still given by (1)-(2). Grid currents are governed with:

$$\begin{aligned} i_{+g} &= \sqrt{2}I\cos(\omega t) \\ i_{-g} &= -\sqrt{2}I\cos(\omega t) \end{aligned} \quad (7)$$

From Fig. 2 it can be seen that grid currents and machine currents have the following correlation:

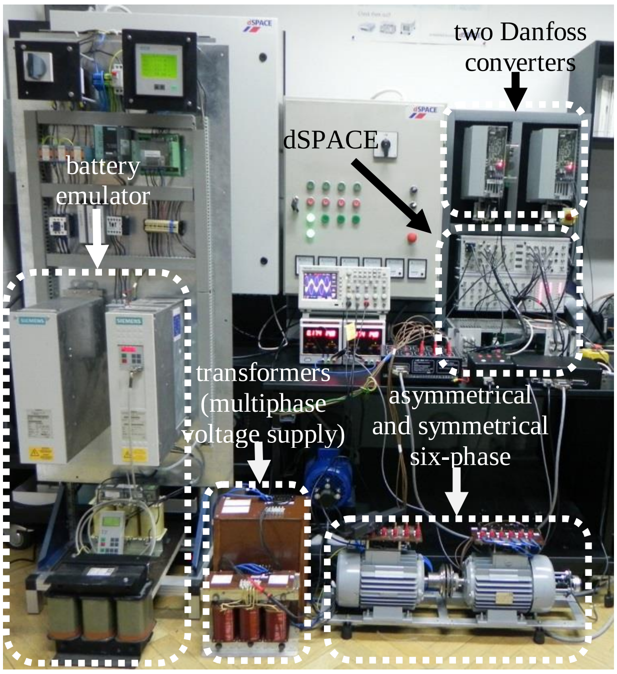

Fig. 5. *Experimental rig.*

$$i_{a1} = i_{b1} = i_{c1} = i_{+g}/3$$
$$i_{a2} = i_{b2} = i_{c2} = i_{-g}/3 \qquad (8)$$

Equations (7)-(8), when substituted into (1), give the following space vectors in the two planes:

$$\underline{i}_{\alpha\beta} = 0 \qquad (9)$$

$$\underline{i}_{xy} = 0 \qquad (10)$$

Zero-sequence components are:

$$i_{0+} = \sqrt{6}(I/3)\cos\omega t$$
$$i_{0-} = -\sqrt{6}(I/3)\cos\omega t \qquad (11)$$

It can be seen that both zero-sequence components exist. They have opposite signs, since the currents through the two three-phase windings flow in opposite directions (and are the same in all phases of any of the two three-phase windings). Total sum of zero-sequence components is zero. The first plane is still without excitation, thus the machine will stay at standstill.

3. EQUIVALENT SCHEMES

Theoretical analysis in Section II demonstrates that asymmetrical six-phase machine, in configurations shown in Fig. 1 and Fig. 2, will not have excitation in torque producing plane during the charging process. This implies that the machine will act as passive resistive-inductive components during the charging process. The equivalent models during the charging mode of operation are presented in Fig. 3 and Fig. 4, respectively.

It can be seen that the topology in Fig. 3 is a multiphase PFC rectifier, while the one in Fig. 4 is a full bridge converter. While the control of single-phase full bridge converter is well known, control of the topology shown in Fig. 3 is less common and can be found in [13]. It should be noted that both topologies can be controlled at unity power factor. Grid currents with very low values of low order harmonics can be achieved, as it will be shown in what follows.

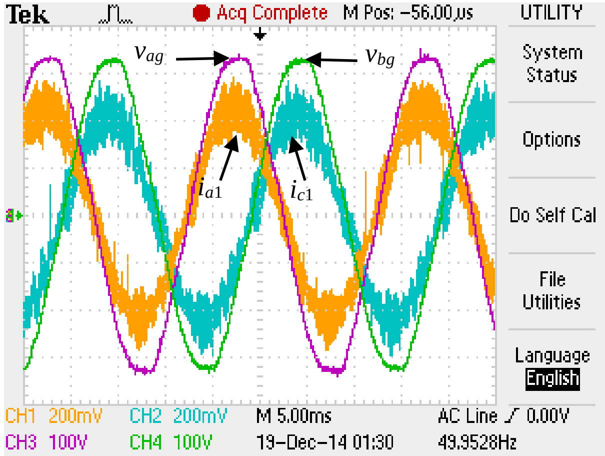

a)

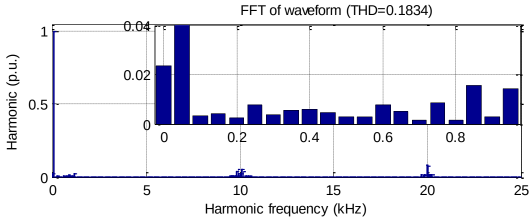

b)

Fig. 6. *Fast charging mode: a) grid phase voltages v_{ag}, v_{bg} and machine currents i_{a1} and i_{c1}, b) spectrum of machine current i_{a1}.*

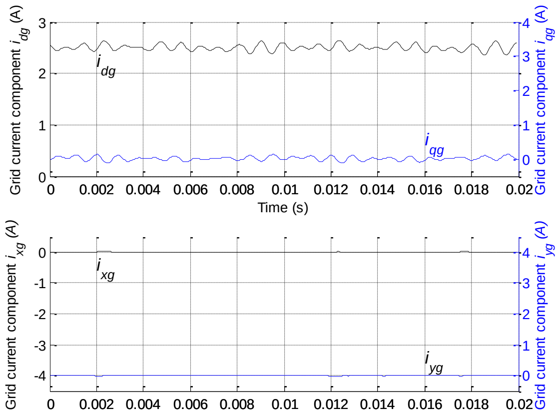

a)

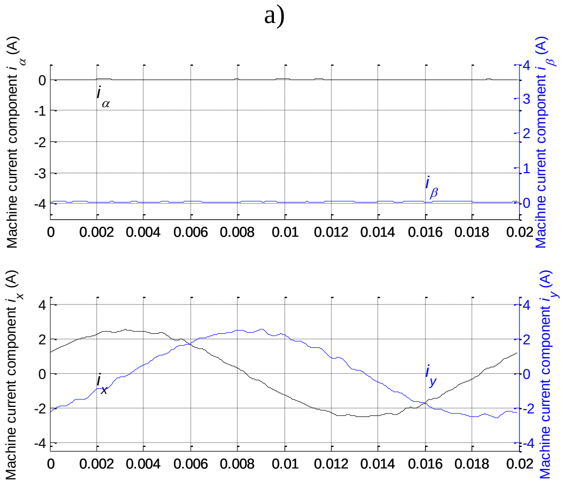

b)

Fig. 7. *Fast charging mode: a) grid current components, b) machine current components - excitation mapping into the two machine's planes.*

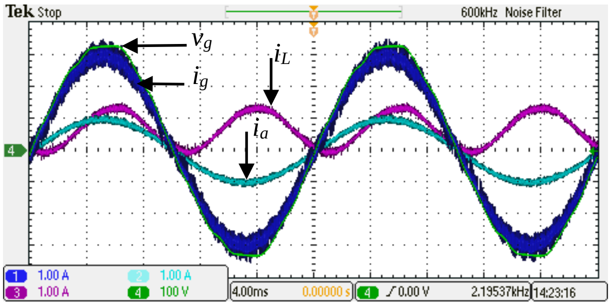

a)

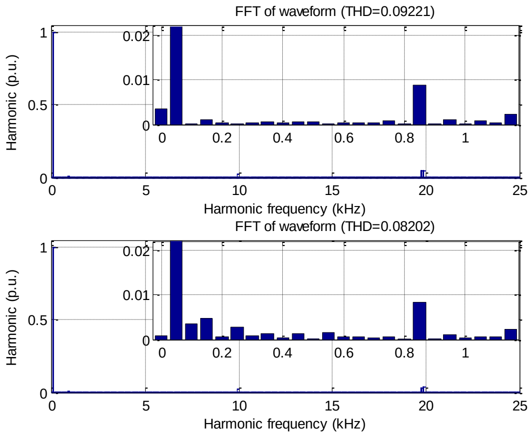

b)

Fig. 8. *Slow charging mode: (a) grid voltage v_g, grid current i_g, machine current i_a and battery charging current i_L, (b) spectra of grid current i_g (upper graph) and machine current i_a (lower graph).*

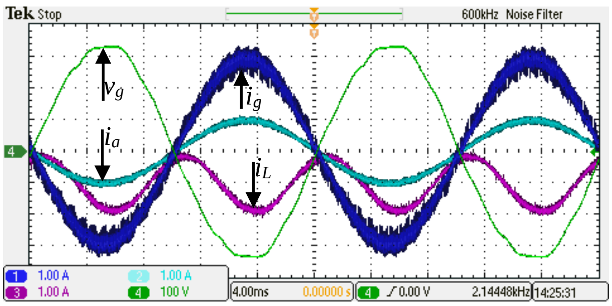

a)

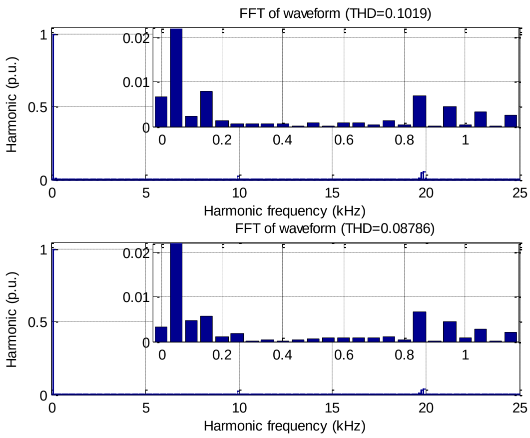

b)

Fig. 9. *Asymmetrical six-phase machine in single-phase V2G mode: (a) grid voltage v_g, grid current i_g, machine current i_a and battery charging current i_L, (b) spectra of grid current i_g (upper graph) and machine current i_a (lower graph).*

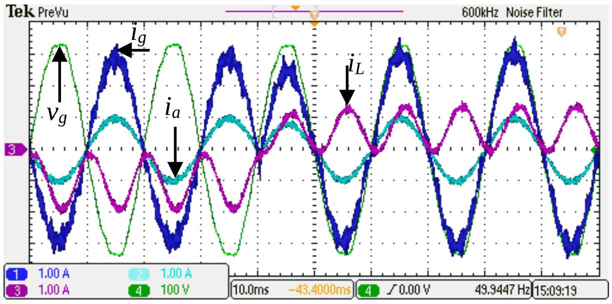

Fig. 10. *Transient from single-phase V2G into charging mode of operation.*

4. EXPERIMENTAL RESULTS

Experiments are performed in order to validate the theory presented in Section 2. Experimental rig is shown in Fig. 5. In order to obtain isolation and asymmetrical six-phase voltage supply, two transformers with connected primary windings are used. A Siemens converter is utilized to emulate a battery and an optional dc-dc converter. Two three-phase Danfoss converters with connected dc-buses are utilized as a six-phase converter. A resistor of a value of 0.5Ω is placed between the Siemens converter and the Danfoss converters in order to emulate battery's internal resistance. Experimental rig data can be found in Appendix and further details are available in [14].

4.1. Fast charging

For the topology of Fig. 3, dc-bus voltage is set to 700 V. The reference for the *d*-component of the grid current is set to the value $i_{dg}^* = 2.5$A for the charging mode. Experimental results are shown in Figs. 6 and 7. From Fig. 6 it can be seen that machine currents are in phase with voltages of the asymmetrical six-phase supply; thus, a unity power factor is achieved. However, machine current i_{c1} is in phase with voltage v_{b1}. This is a consequence of the phase transposition in Fig. 1, as in this topology grid current i_{b1g} and machine current i_{c1} are the same current (Fig. 1). Spectrum of machine current i_{a1} is shown in Fig. 6b, and it demonstrates excellent current quality. Low-order harmonics are below 1% of the fundamental. As a field is not produced in machine's rotor, currents naturally do not contain any unbalance. Indeed, in Fig. 6a the two currents have very similar waveforms.

Fig. 7 is created using experimental data retrieved from the dSPACE system. From Fig. 7a it can be seen that the grid current *d*-component is controlled to its reference ($i_{dg}^* = 2.5$A). The remaining three current components are completely supressed by control. As the *q*-component is kept at zero, unity power factor operation is again verified. In order to assess if a torque is produced during charging/V2G process, machine current components should be observed in a decoupled domain. For the topology of Fig. 1 they are shown in Fig. 7b. Obviously there is no excitation in the torque producing (α-β) plane. As predicted by theoretical analysis (5)-(6), the whole excitation is transferred into the second (non-torque producing) plane. Thus, a torque-free operation is verified, and the machine does not have to be mechanically locked during the charging operation.

4.2. Slow charging

Experiments of single-phase charging are performed using a different (but similar) experimental setup. The grid current amplitude reference is set to 3A. Results of the charging mode are shown in Fig. 8. It is evident that the charging process is performed at unity power factor, since grid currents are in phase with grid voltages. Grid and machine current spectra, shown in upper parts of Figs. 8b, show no low-order harmonics of more than 0.5% of the fundamental. This is a result of proper operation of the current control algorithm, which manages control of the first 15 harmonics.

For V2G mode the current reference is set to -3A, and the results can be seen in Fig. 9. Unity power factor operation is again obvious. If compared with the charging mode (Fig. 8), it can be seen that grid currents have almost the same ripple and spectrum; however, they are now in phase opposition with the voltage. The same is valid for machines' currents.

Finally, by changing the current reference from -3A to 3A in a step-wise manner, a transient from V2G into the charging process is initiated. The obtained results are shown in Fig. 10. It can be seen from the battery charging/discharging current that the energy flow almost instantly changes the direction.

5. CONCLUSION

The paper considers a multiphase topology that is capable of operating as an on-board integrated charger for EVs. It incorporates a six-phase inverter and a six-phase machine into the charging process, and is capable of achieving both single-phase and multiphase charging. A torque is not produced in the machine in either mode. The paper explains the topology and gives detailed equivalent schemes for the two charging configurations. Experimental results are provided to validate the torque-free and unity power factor operation for both fast (multiphase) and slow (single-phase) charging/V2G configurations.

APPENDIX: EXPERIMENTAL EQUIPEMENT DATA

Dc source/sink (battery emulator): Siemens Simovert AFE 6SE7021-3EB81-Z.

Controller: dSPACE containing DS1006 processor board, DS5101 digital waveform output (DWO) board, DS2004 A/D board and DS3001 incremental encoder board.

Converter: Two Danfoss FC302 converters with connected dc-buses. Interface and protection card is added to converters in order to allow a higher degree of controllability.

Asymmetrical six-phase induction machine: the parameters are R_s = 12.8Ω, R_r = 10.5Ω, L_m = 600mH, $L_{\gamma s}$ = $L_{\gamma r}$ = 37.6mH. Obtained by rewinding a 380 V, 50 Hz, 1.1 kW three-phase machine.

6. REFERENCES

[1] J.M. Slicker, "Pulse width modulation inverter with battery charger", *US Patent* 4,491,768, 1985.

[2] S. Haghbin, S. Lundmark, M. Alakula, and O. Carlson, "Grid-connected integrated battery chargers in vehicle applications: review and new solution", *IEEE Trans. on Industrial Electronics*, vol. 60, no. 2, pp. 459-473, 2013.

[3] L. De Sousa, B. Silvestre, and B. Bouchez, "A combined multiphase electric drive and fast battery charger for electric vehicles", *Proc. IEEE Vehicle Power and Propulsion Conference VPPC*, Lille, France, 2010.

[4] S. Haghbin and I. S. Guillen, "Integrated motor drive and non-isolated battery charger based on the torque cancelation in the motor", *IEEE Int. Conf. on Power Electronics and Drive Systems PEDS*, Kitakyushu, Japan, pp. 824-829, 2013.

[5] I. Subotic, N. Bodo, E. Levi, and M. Jones, "On-board integrated battery charger for EVs using an asymmetrical nine-phase machine", *IEEE Trans. on Industrial Electronics*, vol.62, no.5, pp. 3285-3295, 2015.

[6] Renault press kit, "Renault ZOE: the electric supermini for everyday use", www.media.renault.com, February 26, 2013.

[7] I. Subotic and E. Levi, "An integrated battery charger for EVs based on a symmetrical six-phase machine", *IEEE Int. Symposium on Ind. Electronics ISIE*, Istanbul, Turkey, pp. 2074-2079, 2014.

[8] I. Subotic, E. Levi, M. Jones, and D. Graovac, "An integrated battery charger for EVs based on an asymmetrical six-phase machine", *Proc. IEEE Industrial Electronics Society Conf. IECON*, Vienna, Austria, pp. 7242-7247, 2013

[9] I. Subotic, E. Levi, and N. Bodo, "A fast on-board integrated battery charger for EVs using an asymmetrical six-phase machine", *IEEE Vehicle Power and Propulsion Conf. VPPC*, Coimbra, Portugal, pp. 1-6, 2014.

[10] A. P. Sandulescu, F. Meinguet, X. Kestelyn, E. Semail, and A. Bruyere, "Flux-weakening operation of open-end winding drive integrating a cost-effective high-power charger", *IET Electrical Systems in Transportation*, vol. 3, no. 1, pp. 10-21, 2013.

[11] E. Levi, M. Jones, S.N. Vukosavic, and H.A. Toliyat, "A novel concept of a multiphase, multimotor vector controlled drive system supplied from a single voltage source inverter", *IEEE Trans. on Power Electronics*, vol. 19, no. 2, pp. 320- 335, 2004.

[12] E. Levi, R. Bojoi, F. Profumo, H.A. Toliyat, and S. Williamson, "Multiphase induction motor drives - a technology status review", *IET Electric Power Applications*, vol. 1, no. 4, pp. 489-516, 2007.

[13] I. Subotic, N. Bodo, E. Levi, M. Jones, and V. Levi, "Isolated chargers for EVs incorporating six-phase machines," *IEEE Trans. on Industrial Electronics*, 2016, doi: 10.1109/TIE.2015.2412516.

[14] B. Dumnic, D. Milicevic, B. Popadic, V. Katic, and Z. Corba, "Advanced laboratory setup for control of electrical drives as an educational and developmental tool," *Proc. IEEE EuroCon*, Zagreb, Croatia, pp. 903-909, 2013.